Endogenous Endothelins Mediate Increased Distal Tubule Acidification Induced by Dietary Acid in Rats

Donald E. Wesson
Departments of Internal Medicine and Physiology, Texas Tech University Health Sciences Center, Lubbock, Texas 79430

Abstract

We examined if endogenous endothelins mediate the decreased HCO_3 secretion and increased H^+ secretion in in vivo–perfused distal tubules of rats fed dietary acid as $(NH_4)_2SO_4$. Animals given $(NH_4)_2SO_4$ drinking solution had higher endothelin-1 addition to renal interstitial fluid than those given distilled H_2O (480±51 vs. 293±32 fmol g kidney wt^{-1} min$^-$, respectively, $P < 0.03$). $(NH_4)_2SO_4$-ingesting animals infused with bosentan (10 mg/kg) to inhibit A- and B-type endothelin receptors had higher HCO_3 secretion than baseline $(NH_4)_2SO_4$ animals (−4.7±0.4 vs. −2.4±0.3 pmol mm^{-1} min^{-1}, $P < 0.01$), but $(NH_4)_2SO_4$ animals given a specific inhibitor of A-type endothelin receptors (BQ-123) did not (−2.0±0.2 pmol mm^{-1} min^{-1}, P = NS vs. baseline). H^+ secretion was lower in bosentan-infused compared with baseline $(NH_4)_2SO_4$ animals (27.7±2.5 vs. 43.9±4.0 pmol mm^{-1} min^{-1}, $P < 0.03$), but that for BQ-123–infused $(NH_4)_2SO_4$ animals was not (42.9±4.2 pmol mm^{-1} min^{-1}, P = NS vs. baseline). Bosentan had no effect on distal tubule HCO_3 or H^+ secretion in control animals. The data show that dietary acid increases endothelin-1 addition to renal interstitial fluid and that inhibition of B- but not A-type endothelin receptors blunts the decreased HCO_3 secretion and increased H^+ secretion in the distal tubule of animals given dietary acid. The data are consistent with endogenous endothelins as mediators of increased distal tubule acidification induced by dietary acid. (*J. Clin. Invest.* 1997. 99: 2203–2211.) Key words: bicarbonate • bosentan • interstitium • micropuncture • proton • secretion

Introduction

Dietary acid increases acidification in the distal tubule in vivo (1–3), but the factors that induce this response are unknown. This dietary maneuver might increase distal tubule acidification directly through changes in acid–base parameters of body fluids and/or indirectly by altering production of substances that modulate distal tubule acidification. In previous studies from this laboratory, animals ingesting the acid-producing salt $(NH_4)_2SO_4$ increased distal tubule acidification and urine acid excretion without sustained changes in plasma acid–base parameters (3). Furthermore, intracellular pH of cultured renal epithelial cells chronically (48 h) exposed to acid media was not different from control, yet these cells had increased Na^+/H^+ antiporter activity (4). These data suggest that persistent alterations in plasma or intracellular fluid acid–base parameters are not necessary to permit a sustained increase in renal epithelial acidification. Thus, dietary acid might increase distal nephron acidification indirectly by altering production of substances that more directly influence the components of distal tubule acidification. The mechanism by which the distal tubule increases acidification in response to dietary acid might suggest substances responsible for inducing the change. Our previous studies showed that dietary acid decreases HCO_3 secretion and increases H^+-secreting capacity in distal tubules in vivo (3). Endothelin-1 (ET-1),[1] an agent made by collecting tubules (5) and renal microvascular endothelium (6), decreases distal tubule HCO_3 secretion induced by dietary HCO_3 (7) and increases Na^+/H^+ exchanger (NHE)-3 activity in cultured renal epithelia (8). The data show that directional changes in components of distal tubule acidification induced by dietary acid are consistent with ET-1 actions on tubule HCO_3/H^+ secretion.

The present studies used free-flow and in vivo microperfusion micropuncture to test the hypothesis that augmented endothelin secretion mediates increased distal tubule acidification induced by dietary acid. The data show that dietary acid increases ET-1 addition to renal interstitial fluid, a fluid with access to both the renal epithelium and endothelium. Furthermore, the studies show that endothelin receptor inhibition blunts both the decrease in distal tubule HCO_3 secretion and increase in H^+-secreting capacity induced by dietary acid. The data support the hypothesis that endothelin mediates the increase in distal tubule acidification induced by dietary acid.

Methods

Male and female Munich-Wistar rats (Harlan Sprague-Dawley Co., Houston, TX) weighing 240–271 g were used. Previous studies showed that dietary $(NH_4)_2SO_4$ decreased HCO_3 secretion and increased H^+ secreting capacity in the rat distal tubule in vivo (3). We used the same $(NH_4)_2SO_4$-ingesting protocol in the present studies and these animals will be referred to as acid ingesting. Experimental and control animals eating a minimum electrolyte diet (ICN Nutritional Biochemicals, Cleveland, OH) received 40 mM $(NH_4)_2SO_4$ drinking solution and distilled H_2O, respectively, for 7–10 d before micropuncture. Because $(NH_4)_2SO_4$-ingesting animals had higher urine flow than control and because diuresis might increase urine ET-1 excretion (9), we studied a second control group ingesting 40 mM Na_2SO_4 drinking solution that had similar drinking volumes and urine flows to $(NH_4)_2SO_4$ animals. Bosentan (Hoffman-LaRoche, Basel,

Address correspondence to Donald E. Wesson, Texas Tech University Health Sciences Center, Renal Section, 3601 Fourth St., Lubbock, TX 79430. Phone: 806-743-3155; FAX: 806-743-3148; E-mail: phydew@ttuhsc.edu

Received for publication 20 September 1996 and accepted in revised form 20 February 1997.

J. Clin. Invest.

0021-9738/97/05/2203/09 $2.00
Volume 99, Number 9, May 1997, 2203–2211

1. *Abbreviations used in this paper*: ET-1, endothelin-1; J_V, fluid reabsorption; NAE, net acid excretion; NHE, Na^+/H^+ exchanger; RIF, renal interstitial fluid.

Switzerland), a nonpeptide endothelin$_A$ and endothelin$_B$ receptor antagonist (10), was infused (10 mg/kg i.v.) to antagonize actions of endogenous endothelins. This bosentan dose inhibits initial depressor and sustained pressor responses to ET-1 > 60% as long as 6 h (10). To distinguish endothelin$_A$- from endothelin$_B$-mediated effects, we infused a comparison animal group with BQ-123 (Bachem California, Torrence, CA), a selective endothelin$_A$ receptor antagonist (11), 1 mg/kg i.v. followed by 0.1 mg/kg per h. This BQ-123 dose inhibited pressor responses to both stimulated endogenous endothelins and infused ET-1 (12).

Urine net acid excretion. Daily net acid excretion (NAE) was measured as described (13) in four each of control, $(NH_4)_2SO_4$, and Na_2SO_4 animals fed drinking solution and diet as described. Because rats of similar weight ingested 15.6±0.6 g/d of diet when drinking distilled H_2O, 16.7±0.8 g/d for the $(NH_4)_2SO_4$ solution, and 15.9±0.6 g/d for the Na_2SO_4 solution, each animal was fed exactly 15 g/d of diet to ensure that each group ingested the same amount. The diet contained 20% protein and the following electrolytes (in μeq/g diet): 21.7 Na^+, 43.5 K^+, and 13.8 Cl^-. All groups drank distilled H_2O with diet for 48 h, and then were given either 40 mM $(NH_4)_2SO_4$, 40 mM Na_2SO_4, or distilled H_2O (control) for an additional 7 d while in metabolic cages. On each of the subsequent 7 d, animals were anesthetized with ketamine HCl (100 mg/kg body wt; Parke-Davis, Morris Plains, NJ) and bladder urine anaerobically obtained by percutaneous puncture with a 25-gauge needle as done previously (13) for NAE measurement. After anesthesia recovery and excreting blood-free urine, they returned to metabolic cages to continue their drinking solutions. We examined NAE in an additional set of bosentan-infused compared with vehicle-infused animals from each of the three experimental groups after they had ingested their drinking solutions and diet for 7 d. On the evening of the 7th day, animals were anesthetized as described and 10 mg/kg bosentan or vehicle infused into the jugular vein. The wound was closed with surgical clips and NAE was measured as described for the next 12 h.

Microdialysis technique for measurement of renal interstitial fluid ET-1. Renal interstitial fluid (RIF) ET-1 addition was estimated using microdialysis of the renal cortical interstitium (14). A microdialysis apparatus was constructed from a 5-mm-long piece of hollow fiber dialysis tubing (molecular mass cutoff 5,000 D; Hospal, Meyzieu, France) with 0.1-mm inner diameter as described (14). Each end of the dialysis tubing was connected to a 25-cm-long polyethylene tube (0.12-mm inner diameter, 0.65-mm outer diameter; Bioanalytical systems, Indianapolis, IN) and sealed in place with cyanoacrylic glue (14). The left kidney was exposed through a flank incision in anesthetized rats and its renal capsule penetrated with a 31-gauge needle that was tunneled in the outer renal cortex ~ 1 mm from the renal surface for ~ 0.5 mm before exiting by penetrating the renal capsule again. The tip of the needle was inserted into one end of the dialysis probe and pulled together with the dialysis tube until the dialysis fiber was situated within the renal cortex. The flank wound was closed with clips and the inflow tube connected to a gas-tight syringe filled with lactated Ringer's infused at 3 μl/min (Harvard Apparatus, Inc., South Natick, MA), as done by others (14). To quantitate possible contamination of RIF with tubule contents caused by insertion of the microdialysis apparatus, we infused five animals having the microdialysis apparatus in place with a large amount (1 mCi) of ^{3}H-inulin and compared late proximal tubule ^{3}H-inulin concentration with that in RIF as determined by microdialysis. In vitro ^{3}H-inulin recovery, evaluated by immersing dialysis membranes of five identically constructed probes into a beaker containing ^{3}H-inulin, was 89%. RIF ^{3}H-inulin concentration was 4.7% of that in the late proximal tubule, consistent with minimal leakage of tubule contents into RIF. Three consecutive 20-min collection periods were done in four each of control, $(NH_4)_2SO_4$, and Na_2SO_4 animals for RIF ET-1 measurements. In vitro ET-1 recoveries for four identically constructed probes in a beaker with ^{125}I-ET-1 (ICM Biomedicals, Irvine, CA) perfused as described was 59±2%. ET-1 in RIF dialysate was measured using a RIA kit (Peninsula Laboratories Inc., Belmont, CA) after disposable column extraction (Sep-Pak C18; Millipore Corp., Milford, MA) preconditioned with methanol, H_2O, and acetic acid as described (15).

Micropuncture protocol. Animals were prepared for micropuncture of accessible distal tubules as described (16). This distal nephron segment is comprised of multiple epithelia (17) but we will hereafter refer to it as the "distal tubule" for simplicity. Distal tubules were perfused at the early distal flow rate measured in situ (6 nl/min) (18), calibrated in vitro, and verified in vivo (16). Transepithelial potential difference was measured after perfusate collection for each solution (16). An injected latex cast determined perfused tubule length after subsequent acid digestion of the kidney (16). Anaerobically obtained arterial (0.35 ml) and stellate vessel blood plasma (16) was analyzed for tCO_2 using flow-through fluorometry (see below) (19), and for pH, PCO_2, and electrolytes (16). Diet, but not drinking solution, was withheld the evening before studying micropunctured animals, yielding higher baseline HCO_3 reabsorption (20) and permitting differences in HCO_3 reabsorption to be more clearly seen.

Table I depicts perfusate composition. Standard perfusate HCO_3 and Cl^- were 5 and 40 mM, respectively, to approximate these anion concentrations in early distal tubule fluid of control animals (18). Solution 1 contained no HCO_3 to assess blood-to-lumen HCO_3 accumulation and to calculate an apparent transtubule HCO_3 permeability as done previously (16) and described below. Solution 2 was HCO_3- and Cl^--free and contained 0.5 mM acetazolamide. Acetazolamide inhibits HCO_3 (16, 21) and H^+ secretion (22) in the in vivo–perfused rat distal tubule. Thus, measuring luminal HCO_3 accumulation and voltage when perfusing with a zero HCO_3, zero Cl^-, and acetazolamide-containing solution allows calculation of passive blood-to-lumen transepithelial HCO_3 permeability as done in our laboratory (16) and by others (23). Solution 2 was used in this way. Solution 3 contained 5 mM HCO_3 for measurement of net HCO_3 reabsorption and for calculation of luminal H^+ secretion using the apparent transtubule HCO_3 permeability derived from perfusing with solution 1 as described (16). Solution 4 was identical to solution 3 except that it contained 10 rather than 5 mM $NaHCO_3$. This perfusing solution helped to determine if a minimum attainable HCO_3 in distal tubule fluid limited net HCO_3 reabsorption in the $(NH_4)_2SO_4$-ingesting animals as previously reported from this laboratory (3). All perfusing solutions contained raffinose to minimize fluid transport and permit more focused study of HCO_3 transport (16). Three selected distal tubules were perfused in each animal of each group. One distal tubule was perfused with solution 1, another with solution 2, and the third was perfused in paired fashion (16) with solutions 3 and 4 in random order. The order of perfusing solutions was random.

Analytical methods. Immediately after experiment termination, initial and collected perfusate, as well as stellate vessel plasma samples, were analyzed for inulin as done previously (16) and for tCO_2 using flow-through ultrafluorometry (19) as done previously (24). All tubule fluid and plasma tCO_2 were measured on the experimental

Table I. Perfusate Composition in Millimoles

	Solution			
	1	2	3	4
Na^+	61	61	61	61
K^+	4	4	4	4
Cl^-	40	0	40	40
HCO_3	0	0	5	10
Gluconate	25	65	20	15
Acetazolamide	0	0.5	0	0
Raffinose	200	200	200	200

All solutions contained 0.5% FD&C green dye and were equilibrated with 6.7% CO_2.

day by comparing fluorescence of a 7–8-nl sample aliquot (corrected for a distilled H_2O blank run with each sample group) to a standard curve as previously described (24). This technique actually measures tCO_2, but we will refer to this measured value as HCO_3 for simplicity.

Calculations. Net HCO_3 transport was the difference between perfused and collected rates. Net HCO_3 reabsorption refers to net HCO_3 transport obtained when perfusing with initially HCO_3-containing solutions. Luminal HCO_3 accumulation describes net HCO_3 transport obtained when perfusing with initially HCO_3-free solutions. A positive value for HCO_3 transport indicates net HCO_3 movement out of the lumen (reabsorption) and a negative one indicates net HCO_3 movement into the lumen (secretion). A transtubule HCO_3 permeability (P_{HCO3}) was calculated as done previously (16). The term "passive" HCO_3 permeability refers to that obtained when perfusing with zero HCO_3, zero Cl^-, and acetazolamide-containing solution (solution 2). By contrast, the term "apparent" permeability refers to transtubule HCO_3 permeability obtained when perfusing with zero HCO_3, zero Cl^- solution that contained no acetazolamide (solution 1). Bicarbonate secretion was estimated during perfusion with HCO_3-containing solutions by calculating HCO_3 transport into the lumen using the apparent permeability derived from perfusing with the HCO_3-free solution (16). Thus, HCO_3 secretion = apparent permeability × transepithelial HCO_3 gradient corrected for transepithelial potential difference (16). The same apparent permeability (derived perfusing with solution 1 as discussed) was used to calculate HCO_3 secretion when perfusing with both the 5 mM (solution 3) and 10 mM (solution 4) HCO_3-containing solutions. By contrast, a unique transepithelial HCO_3 gradient was calculated for each HCO_3-containing solution using respective tubule HCO_3 concentrations measured when perfusing with that solution (16). The transepithelial potential difference used was the one measured when perfusing with the respective HCO_3-containing solution. H^+ secretion was estimated during perfusion with the HCO_3-containing perfusates by subtracting calculated HCO_3 secretion from measured net HCO_3 reabsorption (16). This method for quantifying H^+ secretion assumes that all HCO_3 transport from the lumen (absolute HCO_3 reabsorption) is mediated by luminal H^+ secretion (22). Furthermore, this method underestimates H^+ secretion to the extent that HCO_3 entering the perfusing solution during perfusion is subsequently reabsorbed. The perfusing solutions contained no NH_3/NH_4^+ for reasons previously discussed (25). Fluid reabsorption (J_v) was the difference between perfused and collected flow rates. All transport values were corrected for perfused tubule length (in mm).

Statistical analysis. The number comprising the three experimental groups represents animals and not tubules. Each reported animal had at least one successful distal tubule perfusion with each perfusing solution. The Bonferroni method was used for *t* test comparison of means ($P < 0.05$) when multiple different comparisons of the same parameter were done in animals among the three animal groups.

Results

General response to dietary protocols. There were no body weight differences between H_2O (control), $(NH_4)_2SO_4$, and Na_2SO_4 animals at the start (255±8, 254±6, and 244±6 g, respectively) or end (268±9, 263±6, and 257±6 g, respectively) of the experimental period. Food intake was not different among groups. Ingested drinking solution volume was higher in $(NH_4)_2SO_4$ (37.1±2.9 ml/d) and Na_2SO_4 (33.2±2.0 ml/d) animals compared with control (21.3±1.8 ml/d, $P < 0.02$ vs. $(NH_4)_2SO_4$ and Na_2SO_4 groups). Similarly, urine flow was higher in $(NH_4)_2SO_4$ (21.1±1.9 ml/d) and Na_2SO_4 (18.2±1.5 ml/d) animals compared with control (11.4±0.9 ml/d, $P < 0.03$ vs. $(NH_4)_2SO_4$ and Na_2SO_4 groups).

Plasma and urine changes induced by drinking solutions. Plasma HCO_3 was not different from the respective baseline value in $(NH_4)_2SO_4$ (25.6±1.4 vs. 25.9±1.4 mM, respectively, P = NS), control (25.5±1.6 vs. 25.7±1.5 mM, respectively, P = NS), or Na_2SO_4 (25.9±1.3 vs. 25.0±1.4 mM, respectively, P = NS) animals. Urine pH decreased compared with its baseline in $(NH_4)_2SO_4$ (5.32±0.06 vs. 6.17±0.05, respectively, $P < 0.001$) and Na_2SO_4 (5.45±0.06 vs. 6.10±0.05, respectively, $P < 0.002$), but not in control (6.15±0.05 vs. 6.16±0.05, respectively, P = NS) animals. Cumulative 7-d NAE was higher in $(NH_4)_2SO_4$ compared with control (42.2±3.1 vs. 19.0±1.8 meq/7 d, respectively, $P < 0.002$), but was not different from control in Na_2SO_4 (24.2±2.1 meq/7 d, $P = 0.22$) animals.

RIF ET-1 addition. Fig. 1 shows higher RIF ET-1 addition in $(NH_4)_2SO_4$ animals compared with control (480±51 vs. 293±32 fmol g kidney wt^{-1} min^{-1}, respectively, $P < 0.05$), but that for Na_2SO_4 animals (275±23 fmol g kidney wt^{-1} min^{-1}) was not different from control.

Effect of endothelin receptor inhibition on systemic blood pressure. Mean blood pressure of micropunctured animals was similar among bosentan-infused, BQ-123–infused, and baseline $(NH_4)_2SO_4$ (110±3, 108±3, and 115±4 mmHg, respectively), control (111±4, 112±3, and 116±3 mmHg, respectively), and Na_2SO_4 animals (107±3, 113±3, and 117±4 mmHg, respectively, P = NS).

Micropuncture data. Because the $(NH_4)_2SO_4$-induced increased urine NAE was accompanied by augmented RIF ET-1 addition, we investigated whether endothelin receptor antagonism in vivo influenced the augmented distal tubule acidification induced by dietary $(NH_4)_2SO_4$ (3). Plasma electrolyte and acid–base composition including arterial and stellate vessel plasma HCO_3 were not different among groups (data not shown). Table II depicts the effect of bosentan, a nonspecific endothelin receptor antagonist (10), and BQ-123, an ET_A selective antagonist (11), on distal tubule HCO_3 transport in situ. In previous studies, $(NH_4)_2SO_4$ animals had lower late distal fluid HCO_3 and lower HCO_3 delivery to this nephron segment than control (3). In the present studies, Table II shows that late distal tubule fluid HCO_3 was higher than baseline in $(NH_4)_2SO_4$ animals given bosentan but not BQ-123. Late distal tubule fluid HCO_3 was higher in bosentan-treated compared with baseline $(NH_4)_2SO_4$ animals despite similar fluid flows (2.0±0.2 vs. 1.8±0.2 nl/min, respectively, P = NS) and tubular fluid-to-plasma inulin ratios (14.1±1.8 vs. 14.8±1.9, respectively, P = NS). By contrast, early and late distal tubule HCO_3 delivery as well as net HCO_3 reabsorption were not different

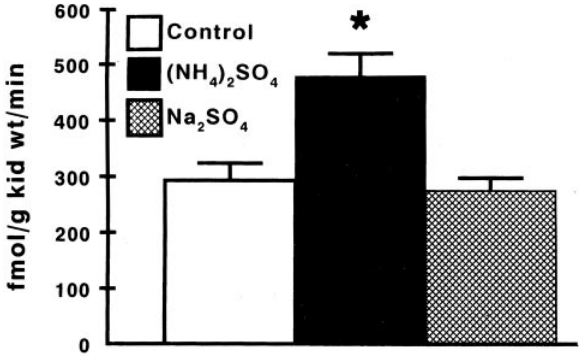

Figure 1. Renal interstitial fluid ET-1 addition in control (*open bar*), $(NH_4)_2SO_4$ (*solid bar*), and Na_2SO_4 (*hatched bar*) animals. *$P < 0.05$ vs. control.

Table II. In Situ tCO_2 Transport in Distal Tubules

	ED HCO_3	LD HCO_3	ED HCO_3 delivery	LD HCO_3 delivery	Net HCO_3 reabsorption
	mM		*pmol/min*		
(NH_4)-SO_4 animals					
$(NH_4)_2SO_4$ ($n = 4$)	5.4±0.3	2.0±0.1	31.9±2.2	3.6±0.5	28.2±2.2
$(NH_4)_2SO_4$ + bosentan ($n = 4$)	5.3±0.3	3.1±0.2*	31.7±2.1	6.2±0.9	25.4±2.0
$(NH_4)_2SO_4$ + BQ-123 ($n = 4$)	5.1±0.3	1.8±0.1	31.0±2.1	3.4±0.4	27.6±2.2
Control animals					
H_2O ($n = 5$)	5.6±0.4	3.9±0.2	34.2±2.5	7.8±1.1	26.5±2.2
H_2O + bosentan ($n = 4$)	5.4±0.3	4.0±0.2	32.4±2.4	8.4±1.2	23.9±2.1
Na_2SO_4 animals					
Na_2SO_4 ($n = 4$)	5.4±0.4	3.4±0.2	32.9±2.3	6.8±0.9	26.0±2.1
Na_2SO_4 + bosentan ($n = 4$)	5.5±0.4	3.8±0.2	33.6±2.5	7.6±1.0	26.1±1.9

Values are means±SEM; ED, early distal tubule; LD, late distal tubule. Chemical designations represent drinking water content. *$P < 0.05$ vs. group without drug.

from baseline in bosentan- or BQ-123–infused $(NH_4)_2SO_4$ animals. Likewise, early distal tubule HCO_3 was similar among $(NH_4)_2SO_4$ animals. Table II shows that in situ distal tubule HCO_3 transport of bosentan-infused animals was not different from baseline in either control or Na_2SO_4 groups.

Decreased luminal HCO_3 induced by dietary acid might increase distal nephron NH_4^+ secretion (28) and thereby increase nephron acid excretion as discussed (3). The bosentan-induced increase in late distal tubule HCO_3 in $(NH_4)_2SO_4$ animals is consistent with an endothelin role in the reduced late distal HCO_3 induced by dietary acid (3). The following studies examined if the bosentan-induced increase in late distal HCO_3 in situ was mediated by increased HCO_3 secretion, decreased H^+ secretion, or both. Data from distal tubules perfused in paired fashion with HCO_3-free solution (solution 1) depicted in Table III were combined with those from paired perfusions with HCO_3-containing solutions 3 and 4 (5 and 10 mM HCO_3, respectively) in Tables V and VI to calculate components of net HCO_3 reabsorption (see Methods). In previous studies, $(NH_4)_2SO_4$ animals had lower luminal HCO_3 accumulation and lower apparent blood-to-lumen HCO_3 permeability than control when perfusing distal tubules with zero-HCO_3 solutions (3). Table III shows higher luminal HCO_3 accumulation and apparent blood-to-lumen HCO_3 permeability in distal tubules of bosentan-treated compared with baseline $(NH_4)_2SO_4$ animals, but these parameters were not different from baseline values in BQ-123–treated $(NH_4)_2SO_4$ animals.

To investigate if the increased luminal HCO_3 accumulation and apparent blood-to-lumen HCO_3 permeability in the bosentan-treated $(NH_4)_2SO_4$ animals was mediated by increased passive blood-to-lumen HCO_3 permeability (see Methods), distal tubules were perfused with an HCO_3- and Cl^--free solution containing acetazolamide (solution 2). Table IV shows that when perfusing with this solution, luminal HCO_3 accumulation and apparent blood-to-lumen HCO_3 permeability were not different between bosentan-treated and baseline $(NH_4)_2SO_4$ animals. These data show that passive blood-to-lumen HCO_3 permeability is similar in bosentan-infused and baseline $(NH_4)_2SO_4$ animals.

The next microperfusion studies investigated the effect of endothelin receptor antagonism on net HCO_3 reabsorption as well as on calculated HCO_3 and H^+ secretion in distal tubules of $(NH_4)_2SO_4$ animals. Table V shows that net HCO_3 reabsorption in bosentan- and BQ-123–treated $(NH_4)_2SO_4$ animals was not different from that of the baseline $(NH_4)_2SO_4$ group when their distal tubules were perfused with the 5-mM HCO_3 solution (solution 3). Fig. 2 shows that calculated HCO_3 secretion (see Methods) was higher in bosentan-infused compared with baseline $(NH_4)_2SO_4$ animals (−4.7±0.5 vs. −2.4±0.3 pmol $mm^{-1}\cdot min^{-1}$, $P < 0.03$), but that for the BQ-123–infused $(NH_4)_2SO_4$ animals was not (−2.0±0.2 pmol $mm^{-1}\cdot min^{-1}$, P = NS). By contrast, Fig. 3 shows that calculated H^+ secretion was not different in the bosentan-infused compared with the baseline $(NH_4)_2SO_4$ animals (22.0±2.0 vs. 24.0±2.1 pmol $mm^{-1}\cdot$

Table III. Net Blood-to-Lumen HCO_3 Fluxes and Permeabilities in Distal Tubules of $(NH_4)_2SO_4$ Animals Perfused with Solution 1 (Zero HCO_3)

Tubule length mm	Flow rate nl/min		HCO_3 mM			PD mV	J_{HCO3} pmol/mm·min^{-1}	Apparent permeability × 10^{-7} cm^2/s
	Perfusion	J_v	Initial	Collected	log mean gradient			
$(NH_4)_2SO_4$ ($n = 4$)								
1.06±0.03	5.9±0.2	0.03±0.01	1.3±0.1	1.8±0.2	28.8±1.2	−13.1±1.2	−2.7±0.3	0.20±0.03
$(NH_4)_2SO_4$ + bosentan ($n = 4$)								
1.08±0.03	6.0±0.2	0.04±0.02	1.2±0.1	2.2±0.2	28.3±1.2	−10.2±1.2	−5.4±0.6*	0.39±0.04*
$(NH_4)_2SO_4$ + BQ-123 ($n = 4$)								
1.02±0.03	5.9±0.2	0.01±0.03	1.3±0.1	1.7±0.2	28.7±1.2	−12.8±1.2	−2.3±0.2	0.17±0.03

Values are means±SEM; chemical designations refer to content of drinking solution. *$P < 0.05$ vs. respective $(NH_4)_2SO_4$ group.

Table IV. Blood-to-Lumen HCO_3 Fluxes and Permeabilities in Distal Tubules of $(NH_4)_2SO_4$ Animals Perfused with Solution 2 (Zero HCO_3, Zero Cl^- with 0.5 mM Acetazolamide)

Tubule length mm	Flow rate nl/min		HCO_3 mM			PD mV	J_{HCO3} pmol/mm·min^{-1}	Passive permeability $\times 10^{-7}$ cm^2/s
	Perfusion	J_v	Initial	Collected	log mean gradient			
$(NH_4)_2SO_4$ (n = 4)								
1.02±0.03	5.9±0.1	−0.01±0.04	1.3±0.1	2.0±0.2	28.7±0.8	−13.7±1.3	−4.1±0.5	0.31±0.04
$(NH_4)_2SO_4$ + bosentan (n = 4)								
1.04±0.03	6.1±0.1	0.04±0.03	1.3±0.1	1.9±0.2	28.4±0.8	−12.5±1.2	−3.4±0.4	0.26±0.03

Values are means±SEM; chemical designations refer to content of drinking solution.

Table V. Bicarbonate Reabsorption by Distal Tubules of $(NH_4)_2SO_4$ Animals Perfused with Solution 3 (5 mM HCO_3)

Tubule length mm	Flow rate nl/min		HCO_3 mM			PD mV	Net HCO_3 reabsorption pmol/mm·min^{-1}
	Perfusion	J_v	Initial	Collected	log mean gradient		
$(NH_4)_2SO_4$ (n = 4)							
1.02±0.03	5.9±0.1	0.03±0.02	5.6±0.3	1.9±0.2	26.6±0.9	−14.2±1.2	21.6±1.8
$(NH_4)_2SO_4$ + bosentan (n = 4)							
1.01±0.03	6.0±0.1	0.01±0.03	5.8±0.3	3.1±0.3	25.5±0.8	−12.2±1.3	17.3±1.6
$(NH_4)_2SO_4$ + BQ-123 (n = 4)							
1.07±0.03	6.1±0.2	0.02±0.01	5.6±0.3	1.7±0.2	26.5±1.0	−14.8±1.5	22.3±1.8

Values are means±SEM; chemical designations refer to content of drinking solution.

min^{-1}, respectively, P = NS). Calculated H^+ secretion was also not different from baseline in BQ-123–infused $(NH_4)_2SO_4$ animals (24.3±2.2 pmol mm^{-1}·min^{-1}, P = NS vs. respective baseline value). Thus, increased HCO_3 secretion contributes to higher late distal tubule HCO_3 of bosentan-infused $(NH_4)_2SO_4$ animals.

The final perfusion studies in $(NH_4)_2SO_4$ animals examined if a minimal attainable HCO_3 might limit measured net HCO_3 reabsorption in distal tubules perfused with HCO_3-containing solutions, limiting calculated H^+ secretion in these animals, and possibly concealing an effect of bosentan on H^+ secretion. Distal tubules were perfused with solution 4, containing a higher initial HCO_3 (10 mM) than solution 3, as discussed earlier. The data are depicted in Table VI. In previous studies, net HCO_3 reabsorption was higher in $(NH_4)_2SO_4$ compared with control animals when distal tubules of each were perfused with 10 mM HCO_3 solution (3). Table VI shows lower net HCO_3 reabsorption in distal tubules of bosentan-infused but not BQ-123–infused $(NH_4)_2SO_4$ animals. H^+ and HCO_3 secretion for the 10-mM HCO_3 perfusions were calculated as for the 5-mM HCO_3 perfusions, using apparent permeability derived from the perfusion with solution 1 (see Methods). Fig. 4 shows that calculated HCO_3 secretion was higher in distal tubules of the bosentan-infused compared with the baseline $(NH_4)_2SO_4$ animals perfused with 10 mM HCO_3 (−3.9±0.4 vs. −2.0±0.2 pmol mm^{-1}·min^{-1}, $P < 0.05$), but that for the BQ-123–infused $(NH_4)_2SO_4$ animals was not (−1.7±0.2 pmol mm^{-1}·min^{-1}, P = NS). In contrast with the findings described when perfusing with the 5-mM HCO_3 solutions, Fig. 5 shows that bosentan-infused $(NH_4)_2SO_4$ animals had lower calculated H^+ secretion compared with the baseline value (27.7±2.5 vs. 43.9±4.0 pmol mm^{-1}·min^{-1}, $P < 0.05$). H^+ secretion in distal tubules of BQ-123–infused $(NH_4)_2SO_4$ animals was not different from the baseline value (42.9±4.2 pmol mm^{-1}·min^{-1}, P = NS). Thus,

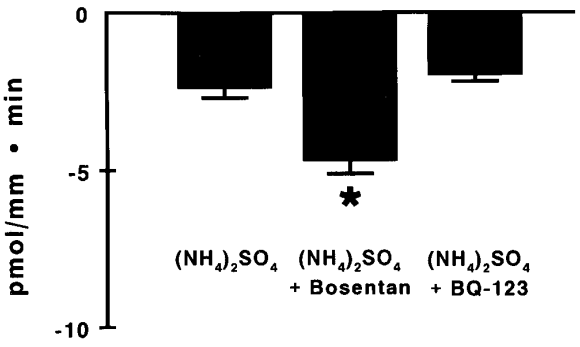

Figure 2. Bicarbonate secretion by distal tubules perfused with solution 3 (5 mM HCO_3) in $(NH_4)_2SO_4$-ingesting animals at baseline and after bosentan (10 mg/kg) or BQ-123 (1 mg/kg bolus followed by 0.1 mg kg^{-1} min^{-1}) infusion. *$P < 0.05$ vs. $(NH_4)_2SO_4$ (baseline) group.

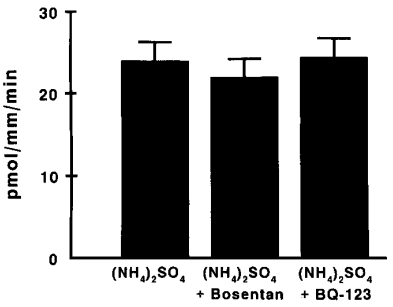

Figure 3. Proton secretion by distal tubules perfused with solution 3 (5 mM HCO_3) in $(NH_4)_2SO_4$-ingesting animals at baseline and after infusion of bosentan (10 mg/kg) or BQ-123 (1 mg/kg bolus followed by 0.1 mg kg^{-1} min^{-1}).

Table VI. Bircarbonate Reabsorption by Distal Tubules $(NH_4)_2SO_4$ Animals Perfused with Solution 4 (10 mM HCO_3)

Tubule length mm	Flow rate nl/min		HCO_3 mM			PD mV	Net HCO_3 reabsorption pmol/mm·min^{-1}
	Perfusion	J_v	Initial	Collected	log mean gradient		
$(NH_4)_2SO_4$ (n = 3)							
0.96±0.03	5.9±0.2	0.01±0.03	11.3±0.2	4.5±0.2*	22.3±1.0	−15.0±1.4	41.9±3.8
$(NH_4)_2SO_4$ + bosentan (n = 4)							
1.03±0.04	6.2±0.3	0.05±0.04	11.2±0.3	7.3±0.3*	21.7±1.1	−12.9±1.3	23.8±2.5*
$(NH_4)_2SO_4$ + BQ-123 (n = 3)							
0.98±0.03	6.0±0.2	0.04±0.02	11.1±0.2	4.4±0.2	22.3±1.1	−15.1±1.5	41.2±4.2

Values are means±SEM; chemical designations refer to content of drinking solution. *$P < 0.05$ vs. respective $(NH_4)_2SO_4$ group.

Table VII. Net Blood-to-Lumen HCO_3 Fluxes and Permeabilities in Distal Tubules of Control Animals Perfused with Solution 1 (Zero HCO_3)

Tubule length mm	Flow rate nl/min		HCO_3 mM			PD mV	J_{HCO3} pmol/mm·min^{-1}	Apparent permeability × 10^{-7} cm^2/s
	Perfusion	J_v	Initial	Collected	log mean gradient			
H_2O (n = 5)								
1.03±0.03	5.9±0.2	0.01±0.03	1.3±0.1	2.3±0.2	31.7±1.2	−12.9±1.3	−5.7±0.8	0.39±0.05
H_2O + bosentan (n = 4)								
1.05±0.04	5.9±0.1	0.02±0.02	1.2±0.1	2.4±0.2	31.7±1.3	−12.4±1.2	−6.6±0.7	0.44±0.05

Values are means±SEM; chemical designations refer to content of drinking solution.

decreased H^+ secretory capacity contributes to higher HCO_3 at the late distal tubule in situ of bosentan-infused $(NH_4)_2SO_4$ animals.

We next examined the effect of bosentan on HCO_3 transport in control animals. Table VII shows no difference in luminal HCO_3 accumulation or apparent permeability between bosentan-infused and baseline controls perfused with solution 1 (zero HCO_3). Because differences in net HCO_3 reabsorption between $(NH_4)_2SO_4$ animals and control were evident perfusing with the 10 but not 5 mM HCO_3 solution, the 10-mM solution (solution 4) was perfused in distal tubules of control animals to determine if bosentan influenced net HCO_3 reabsorption and/or its components (HCO_3/H^+ secretion) in control animals. Table VIII shows that net HCO_3 reabsorption was not different between bosentan-infused and baseline control animals perfused with 10 mM HCO_3. Calculated secretion of HCO_3 (−5.0±0.6 vs. −4.4±0.5 pmol mm^{-1}·min^{-1}, P = NS) and H^+ (20.2±2.0 vs. 23.2±2.2 pmol mm^{-1}·min^{-1}, P = NS) were also not different in bosentan-infused and baseline controls, respectively. Thus, endothelin receptor antagonism did not affect distal tubule acidification in control animals.

The final series of microperfusion studies determined if bosentan influenced distal tubule HCO_3 transport in Na_2SO_4 animals, a group whose urine flow was higher than control but comparable to that for $(NH_4)_2SO_4$ animals. This higher urine flow might itself increase urine ET-1 excretion (9) and thereby influence distal tubule acidification independent of dietary acid intake. Table IX shows no difference in luminal HCO_3 accumulation or apparent permeability between bosentan-infused and baseline Na_2SO_4 animals perfused with solution 1 (zero HCO_3). As with the control animals, the 10-mM HCO_3 solution (solution 4) was used in distal tubules of Na_2SO_4 animals

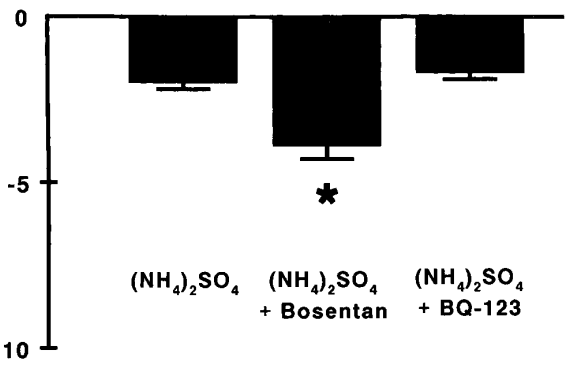

Figure 4. Bicarbonate secretion by distal tubules perfused with solution 4 (10 mM HCO_3) in $(NH_4)_2SO_4$-ingesting animals at baseline and after infusion of bosentan (10 mg/kg) or BQ-123 (1 mg/kg bolus followed by 0.1 mg kg^{-1} min^{-1}). *$P < 0.05$ vs. $(NH_4)_2SO_4$ (baseline) group.

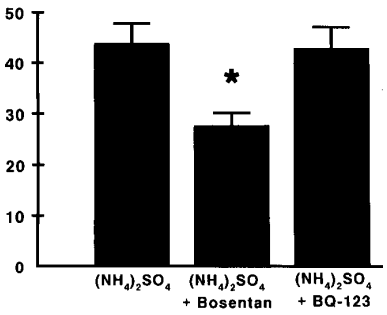

Figure 5. Proton secretion by distal tubules perfused with solution 4 (10 mM HCO_3) in $(NH_4)_2SO_4$-ingesting animals at baseline and after infusion of bosentan (10 mg/kg) or BQ-123 (1 mg/kg bolus followed by 0.1 mg kg^{-1} min^{-1}). *$P < 0.05$ vs. $(NH_4)_2SO_4$ (baseline) group.

Table VIII. Bicarbonate Reabsorption by Distal Tubules of Control Animals Perfused with Solution 4 (10 mM HCO_3)

Tubule length mm	Flow rate nl/min		HCO_3 mM			PD mV	Net HCO_3 reabsorption pmol/mm·min^{-1}
	Perfusion	J_v	Initial	Collected	log mean gradient		
H_2O (n = 4)							
1.04±0.03	5.9±0.1	0.01±0.03	10.6±0.5	7.3±0.3	24.5±1.3	−13.2±1.5	18.8±1.9
H_2O + bosentan (n = 4)							
1.02±0.03	5.9±0.1	0.01±0.03	10.3±0.4	7.7±0.3	24.5±1.3	−12.8±1.2	15.1±1.5

Values are means±SEM; chemical designations refer to content of drinking solution.

Table IX. Net Blood-to-Lumen HCO_3 Fluxes and Permeabilities in Distal Tubules of Na_2SO_4 Animals Perfused with Solution 1 (Zero HCO_3)

Tubule length mm	Flow rate nl/min		HCO_3 mM			PD mV	J_{HCO3} pmol/mm·min^{-1}	Apparent permeability $\times 10^{-7}$ cm^2/s
	Perfusion	J_v	Initial	Collected	log mean gradient			
Na_2SO_4 (n = 4)								
0.93±0.04	5.9±0.2	−0.03±0.01	1.3±0.1	2.0±0.2	30.3±1.1	−16.2±1.5	−4.5±0.6	0.34±0.05
Na_2SO_4 + bosentan (n = 4)								
0.97±0.04	6.1±0.2	0.04±0.02	1.4±0.1	2.2±0.2	30.0±1.1	−15.1±1.3	−5.2±0.7	0.38±0.05

Values are means±SEM; chemical designations refer to content of drinking solution.

to determine if bosentan influenced net HCO_3 reabsorption and/or its components in this group. Table X shows that net HCO_3 reabsorption was not different between bosentan-infused and baseline Na_2SO_4 animals. Calculated secretion of HCO_3 (−3.8±0.5 vs. −3.4±0.4 pmol mm^{-1}·min^{-1}, P = NS) and H^+ (23.8±2.2 vs. 29.4±2.6 pmol mm^{-1}·min^{-1}, P = NS) were also not different in bosentan-infused and baseline Na_2SO_4 animals, respectively. Thus, endothelin receptor antagonism did not affect distal tubule acidification in Na_2SO_4 animals.

Effect of endothelin receptor inhibition on NAE. Because bosentan decreased acidification in the distal tubule of $(NH_4)_2SO_4$ animals, we investigated if this receptor antagonist reduced NAE. 12-h NAE after administration of the same bosentan dose (10 mg/kg i.v.) that had been given to micropunctured animals was not different in bosentan-infused compared with vehicle-infused $(NH_4)_2SO_4$ (3.2±0.5 vs. 4.1±0.6 meq/12 h, respectively, P = NS), control (1.7±0.3 vs. 1.7±0.2 meq/12 h, respectively, P = NS), or Na_2SO_4 (1.7±0.2 vs. 1.8±0.2 meq/12 h, respectively, P = NS) animals.

Discussion

Many investigations employing a variety of techniques have defined effector mechanisms by which the kidney increases acidification in response to dietary acid (26). Such investigations show an important role of increased distal nephron acidification in this response (1–3, 27–29). The distal tubule of animals ingesting dietary acid have augmented H^+ secreting capacity (1–3) and reduced HCO_3 delivery to the terminal distal nephron (3, 30), the latter facilitating increased titration of non-HCO_3 buffers (28, 31). Recent studies from our laboratory show that reduced distal tubule HCO_3 secretion contributes to the decreased terminal distal nephron HCO_3 delivery induced by dietary acid (3). Thus, dietary acid alters both components of distal tubule net HCO_3 reabsorption (H^+/HCO_3 secretion) in a direction that increases acidification, but the immediate stimulus that induces this response is not known. Much less is understood about the mechanisms that induce distal nephron epithelia to respond in this way to a dietary acid challenge. Dietary acid–induced alterations in body fluid acid–

Table X. Bicarbonate Reabsorption by Distal Tubules of Na_2SO_4 Animals Perfused with Solution 4 (10 mM HCO_3)

Tubule length mm	Flow rate nl/min		HCO_3 mM			PD mV	Net HCO_3 reabsorption pmol/mm·min^{-1}
	Perfusion	J_v	Initial	Collected	log mean gradient		
Na_2SO_4 (n = 4)							
1.01±0.05	6.1±0.1	0.05±0.03	10.9±0.5	6.7±0.4	23.1±1.3	−15.9±1.5	25.6±2.3
Na_2SO_4 + bosentan (n = 4)							
0.98±0.03	5.8±0.2	−0.04±0.02	10.7±0.6	7.2±0.4	22.8±1.3	−15.8±1.6	20.4±1.8

Values are means±SEM; chemical designations refer to content of drinking solution.

base parameters might increase distal nephron acidification directly. Although changes in environmental acid–base parameters can induce predictable alterations in acidification of renal epithelia studied in vitro (32, 33), it is clear that sustained changes in plasma (3, 24) or intracellular (4) acid–base parameters are not necessary to maintain altered renal epithelial acidification (3, 4, 24). Alternative or additional mechanisms include diet-induced modification of the level and/or activity of secretory substances that modify renal epithelial acidification. The present studies tested the hypothesis that endothelin mediates increased distal tubule acidification induced by dietary acid. This hypothesis derives from studies showing that ET-1 increases NHE-3 activity in cultured renal epithelial cells (8) and decreases distal tubule HCO_3 secretion induced by dietary HCO_3 (7). The data show that animals given dietary acid have greater ET-1 addition to RIF. Furthermore, B- but not A-type endothelin receptor inhibition blunts decreased HCO_3 secretion and increased H^+-secreting capacity induced by dietary acid. Endothelin receptor inhibition had no measurable effect on distal tubule acidification in control animals, suggesting that endothelin contributes less to the "tonic" level of distal tubule acidification under control conditions. The data support the hypothesis that endothelin mediates increased distal tubule acidification induced by dietary acid.

Although the endothelins were initially noted for their vasoactive effects (34), these agents also modulate epithelial transport by inhibiting the amiloride-sensitive Na^+ channel (35) and ADH-mediated H_2O reabsorption (36) in collecting tubules. ET-1 also stimulates the Na^+/H^+ exchanger in renal cortical membrane vesicles (37) and the NHE-3 isoform in renal epithelial cells (8), supporting a possible endothelin role in modulating renal acidification in vivo. The NHE performs much of the H^+ secretion in the rat distal tubule accessible to micropuncture (38). ET-1 also inhibits agonist-stimulated increases in cellular cyclic AMP levels in renal epithelium (36), a cellular second messenger whose increase is associated with augmented HCO_3 secretion in cortical collecting tubules (39) and with inhibited NHE activity in renal brush border membranes (40). Preliminary studies show that ET-1 decreases distal tubule HCO_3 secretion induced by dietary HCO_3 (7), an important response to this dietary maneuver (24). By contrast, ET-1 inhibited net HCO_3 reabsorption in proximal straight tubules (41), suggesting distinct ET-1 effects on acidification in this nephron segment. The present studies show that endothelin receptor inhibition blunts decreased HCO_3 secretion and increased H^+ secretion in the distal tubule induced by dietary acid (3). The data suggest that endogenous endothelins mediate the decreased HCO_3 secretion and increased H^+ secretion induced by dietary acid.

The present studies show that dietary acid increases ET-1 addition to RIF, a fluid compartment in direct communication with basolateral surfaces of cortical renal epithelium. This anatomical arrangement would permit endothelins secreted into RIF to modulate cortical epithelial transport through endothelin receptors on the surface of cultured canine cells of distal nephron origin (42). Furthermore, rat cortical collecting tubules contain mRNA for the B-type endothelin receptor (43), which the present studies suggest mediates the described actions of endogenous endothelins. Endothelins in the RIF might derive from collecting tubule epithelium (5) or endothelium of the renal microvasculature (6, 44). The latter is separated from distal tubules in vivo by only a very narrow interstitial space (45), permitting paracrine or autocrine communication among cell types. In addition, microdissected cortical collecting tubules contain ET-1 mRNA (43, 46), and ET-1 is on the endothelial surfaces of peritubular capillaries (44). The present studies show that dietary acid increases RIF ET-1 addition and suggest that the added ET-1 subsequently increases distal tubule acidification.

Calculated HCO_3 and H^+ secretion were not different in bosentan-infused control animals, in contrast with the $(NH_4)_2SO_4$ animals in which bosentan increased HCO_3 secretion and decreased H^+ secretory capacity. Although a higher bosentan dose might influence control HCO_3/H^+ secretion, the data suggest that endogenous endothelins have a greater influence on basal distal tubule acidification in acid-ingesting compared with control animals. By contrast, endogenous endothelins apparently contribute less than intrinsic, neural, or other autocrine/paracrine mechanisms to basal distal tubule acidification. Nevertheless, the same bosentan dose that reduced distal nephron acidification in $(NH_4)_2SO_4$ animals did not reduce augmented NAE in these animals. This suggests less endothelin effect on acidification and/or less sensitivity to the administered bosentan dose in more terminal nephron segments.

The present studies support that endogenous endothelins inhibit distal tubule HCO_3 secretion and stimulate H^+ secretion in this nephron segment, but do not indicate the cellular signaling mechanisms that mediate these effects. Increased cellular cAMP levels are associated with stimulated HCO_3 secretion by the collecting tubule (39) and with inhibited Na^+/H^+ exchange in brush border membranes (40). In addition, ET-1 inhibits agonist-induced increases in cortical collecting tubule cAMP (36), complimenting the ET-1 effects on distal tubule HCO_3 secretion. Furthermore, prostacyclin (PGI_2), an agent that increases cellular cAMP levels in distal nephron epithelia (47), increases distal tubule HCO_3 secretion (48). Yet, ET-1 also stimulates Ca^{2+} release from internal stores and its entry into cortical collecting duct cells (49), consistent with activation of phospholipase C (50). In addition, activation of the B-type endothelin receptor leads to generation of nitric oxide through a tyrosine kinase–dependent and Ca^{2+}/calmodulin-dependent pathway (51). Thus, ET-1 might alter HCO_3/H^+ secretion by these and possibly other mechanisms.

In summary, the present studies show that reduced HCO_3 secretion and increased H^+ secretory capacity in the distal tubule induced by dietary acid is associated with increased ET-1 addition to RIF. Furthermore, inhibition of B- but not A-type endothelin receptors blunts the reduced HCO_3 secretion and increased H^+ secretory capacity induced by dietary acid, but does not affect distal tubule acidification in control animals. The data suggest that endogenous endothelins mediate increased distal tubule acidification induced by dietary acid but contribute less to basal acidification in this segment.

Acknowledgments

We are grateful to Mrs. Geraldine Tasby and Ms. Cathey Hudson for expert technical assistance, and to Neil A. Kurtzman for his continued support. We are also grateful to Martine Clozel, M.D. for generously providing bosentan, without which these studies would not have been possible.

This work was supported by funds from National Institutes of Health grant 5-RO1-DK 36199-10 (N.A. Kurtzman, principle investigator) and from the Texas Tech University Health Sciences Center.

References

1. Levine, D.Z. 1985. An in vivo microperfusion study of distal tubule bicarbonate reabsorption in normal and ammonium chloride rats. *J. Clin. Invest.* 75: 588–595.

2. Kunau, R.T., and K.A. Walker. 1987. Total CO_2 absorption in the distal tubule of the rat. *Am. J. Physiol.* 252:F468–F473.

3. Wesson, D.E. 1996. Reduced bicarbonate secretion mediates increased distal tubule acidification induced by dietary acid. *Am. J. Physiol.* 271:F670–F678.

4. Horie, S., O. Moe, A. Tejedor, and R.J. Alpern. 1990. Preincubation in acid medium increases Na/H antiporter activity in cultured renal proximal tubule cells. *Proc. Natl. Acad. Sci. USA.* 87:4742–4745.

5. Kohan, D.E. 1991. Endothelin synthesis by rabbit renal tubule cells. *Am. J. Physiol.* 261:F221–F226.

6. Wesson, D.E., J. Simoni, and D.F. Green. 1996. Acidic extracellular pH increases Endothelin-1 secretion by human endothelial cells of glomerular but not aortic origin. *J. Invest. Med.* 44:336*a*. (Abstr.)

7. Wesson, D.E., and G.M. Dolson. 1996. Endothelin inhibits distal tubule HCO_3 secretion induced by dietary HCO_3. American Physiological Society Conference, Snowmass, CO. July 12–14. (Abstr.)

8. Chu, T.-S., Y. Peng, A. Cano, M. Yanagisawa, and R.J. Alpern. 1996. Endothelin$_B$ receptor activates NHE-3 by a Ca^{2+}-dependent pathway in OKP cells. *J. Clin. Invest.* 97:1454–1462.

9. Zeiler, M., B.M. Loffler, H.A. Block, and G. Thiel. 1995. ET-1 excretion is flow-dependent in kidney donors and transplant recipients. *J. Cardiovasc. Pharmacol.* 26(Suppl. 3):S513–S515.

10. Clozel, M., V. Breu, G. Gray, B. Kalina, B.-M. Loffler, K. Burri, J.-M. Cassal, G. Hirth, M. Muller, W. Neidhart, and H. Ramuz. 1994. Pharmacological characterization of Bosentan, a new potent orally active nonpeptide endothelin receptor antagonist. *J. Pharmacol. Exp. Ther.* 270:228–235.

11. Ihara, M., K. Noguchi, T. Fukuroda, S. Tsuchida, S Kimura, T. Fukami, K. Ishikawa, M. Nishikibe, and M. Yano. 1992. Biological profiles of highly potent novel endothelin antagonists selective for the ETA receptor. *Life Sci.* 50: 247–255.

12. Kivlighn, S.D., R.A. Gabel, and P.K.S. Siegl. 1994. Effects of BQ-123 on renal function and acute cyclosporin-induced renal dysfunction. *Kidney Int.* 45: 131–136.

13. Wesson, D.E. 1990. Dietary bicarbonate reduces rat distal nephron acidification evaluated in situ. *Am. J. Physiol.* 258:F870–F876.

14. Siragy, H.M., M.M. Ibrahim, A.A. Jaffa, R. Mayfield, and H.S. Margolius. 1994. Rat renal interstitial bradykinin, prostaglandin E_2, and cyclic guanosine 3′, 5′-monophosphate. Effects of altered sodium intake. *Hypertension (Dallas).* 23:1068–1070.

15. Benigni, A., N. Perico, F. Gaspari, C. Zoja, L. Bellizzi, M. Gabanelli, and G. Remuzzi. 1991. Increased renal endothelin production in rats with reduced renal mass. *Am. J. Physiol.* 260:F331–F339.

16. Wesson, D.E., and G.M. Dolson. 1991. Augmented bidirectional HCO_3 transport by rat distal tubules in chronic alkalosis. *Am. J. Physiol.* 261:F308–F317.

17. Crayen, M.L., and W. Thoenes. 1978. Architecture and cell structures in the distal nephron of the rat kidney. *Cytobiologie.* 17:197–211.

18. Wesson, D.E. 1990. Depressed distal tubule acidification corrects chloride-deplete alkalosis in rats. *Am J. Physiol.* 259:F636–F644.

19. Star, R.A. 1990. Quantitation of total carbon dioxide in nanoliter samples by flow-through fluorometry. *Am J. Physiol.* 258:F429–F432.

20. Levine, D.Z., M. Iacovitti, L. Nash, and D. Vandorpe. 1988. Secretion of bicarbonate by rat distal tubules in vivo. Modulation by overnight fasting. *J. Clin. Invest.* 81:1873–1878.

21. Iacovitti, M., L. Nash, L.N. Peterson, J. Rochon, and D.Z. Levine. 1986. Distal tubule bicarbonate accumulation in vivo. Effect of flow and transtubular bicarbonate gradients. *J. Clin. Invest.* 78:1658–1665.

22. Capasso, G., R. Kinne, G. Malnic, and G. Giebisch. 1986. Renal bicarbonate reabsorption in the rat. I. Effects of hypokalemia and carbonic anhydrase. *J. Clin. Invest.* 78:1558–1567.

23. Chan, Y.L., G. Malnic, and G. Giebisch. 1989. Renal bicarbonate reabsorption in the rat. III. Distal tubule perfusion study of load dependence and bicarbonate permeability. *J. Clin. Invest.* 84:931–938.

24. Wesson, D.E. 1996. Dietary HCO_3 reduces distal tubule acidification by increasing cellular HCO_3 secretion. *Am J. Physiol.* 271:F132–F142.

25. Wesson, D.E., and G.M. Dolson. 1991. Maximal proton secretory rate of rat distal tubules is higher during chronic metabolic alkalosis. *Am. J. Physiol.* 261:F753–F759.

26. Levine, D., and H.R. Jacobson. 1986. The regulation of renal acid secretion: new observations from studies of distal nephron segments. *Kidney Int.* 29: 1099–1109.

27. Garcia-Austt, J., D.W. Good, M.B. Burg, and M.A. Knepper. 1985. Deoxycorticosterone-stimulated bicarbonate secretion in rabbit cortical collecting ducts: effects of luminal chloride removal and in vivo acid loading. *Am. J. Physiol.* 249:F205–F212.

28. Knepper, M.A., D.W. Good, and M.B. Burg. 1985. Ammonia and bicarbonate transport by rat cortical collecting ducts perfused in vitro. *Am. J. Physiol.* 249:F870–F877.

29. Lucci, M.S., L.R. Pucacco, N.W. Carter, and T.D. DuBose, Jr. 1982. Evaluation of bicarbonate transport in the rat distal tubule: effects of acid-base status. *Am. J. Physiol.* 243:F335–F341.

30. Buerkert, J., D. Martin, and D. Trigg. 1983. Segmental analysis of the renal tubule in buffer production and net acid formation. *Am. J. Physiol.* 244: F442–F454.

31. Knepper, M.A., R. Packer, and D.W. Good. 1989. Ammonium transport in the kidney. *Physiol. Rev.* 69:179–248.

32. Breyer, M.D., J.P. Kokko, and H.R. Jacobson. 1986. Regulation of net bicarbonate transport in rabbit cortical collecting tubule by peritubular pH, carbon dioxide tension, and bicarbonate concentration. *J. Clin. Invest.* 77:1650–1660.

33. McKinney, T.D., and K.K. Davidson. 1988. Effects of respiratory acidosis on HCO_3 transport by rabbit collecting tubules. *Am. J. Physiol.* 255:F656–F665.

34. Marsen, T.A., H. Schramek, and M.J. Dunn. 1994. Renal actions of endothelin. Linking cellular signaling pathways to kidney disease. *Kidney Int.* 45: 336–344.

35. Ling, B.N. 1995. Effect of luminal endothelin-1 on apical Na^+ and Cl^- channels in primary cultured rabbit CCT. *Clin. Res.* 43:47α. (Abstr.)

36. Tomita, K., H. Nonguchi, and F. Marumo. 1990. Effects of endothelin on peptide-dependent cyclic adenosine monophosphate accumulation along the nephron segments of the rat. *J. Clin. Invest.* 85:2014–2018.

37. Eiam-Ong, S., S.A. Hilden, A.J. King, C.A. Johns, and N.E. Madias. 1992. Endothelin-1 stimulates the Na^+/H^+ and Na^+/HCO_3^- transporters in rabbit renal cortex. *Kidney Int.* 42:18–24.

38. Wang, T.G., G. Malnic, G. Giebisch, and Y.L. Chan. 1993. Renal bicarbonate reabsorption in the rat. IV. Bicarbonate transport mechanisms in the early and late distal tubule. *J. Clin. Invest.* 91:2776–2883.

39. Emmons, C., and J.B. Stokes. 1994. Cellular actions of cAMP on HCO_3^--secreting cells of rabbit CCD: dependence on in vivo acid-base status. *Am. J. Physiol.* 266:F528–F535.

40. Weinman, E.J., S. Shenolikar, and A.M. Kahn. 1987. cAMP-associated inhibition of Na^+-H^+ exchanger in rabbit kidney brush border membranes. *Am. J. Physiol.* 252:F19–F25.

41. Garvin, J., and K. Sanders. 1991. Endothelin inhibits fluid and bicarbonate transport in part by reducing Na^+/K^+ ATPase activity in the rat proximal straight tubule. *J. Am. Soc. Nephrol.* 2:976–982.

42. Neuster, D., S. Zaiss, and J.-P. Stasch. 1990. Endothelin receptors in cultured renal epithelial cells. *Eur. J. Pharmacol.* 176:241–243.

43. Terada, Y., K. Tomita, H. Nonoguchi, and F. Marumo. 1992. Different localization of two types of endothelin receptor mRNA in microdissected rat nephron segments using reverse transcription and polymerase chain reaction assay. *J. Clin. Invest.* 90:107–112.

44. Wilkes, B.M., M. Susin, P.F. Mento, C.M. Macica, E.P. Giraldi, E. Boss, and E.P. Nord. 1991. Localization of endothelin-like immunoreactivity in rat kidneys. *Am J. Physiol.* 260:F913–F920.

45. Kriz, W., and B. Kaissling. 1992. Structural organization of the mammalian kidney. *In* The Kidney. Physiology and Pathophysiology. D. Seldin and G. Giebisch, editors. Raven Press, New York. p. 207.

46. Uchida, S., F. Takemoto, E. Ogata, and K. Kuroka. 1992. Detection of endothelin-1 mRNA by RT-PCR in isolated rat renal tubules. *Biochem. Biophys. Res. Commun.* 188:108–113.

47. Veis, J.H., M.A. Dillingham, and T. Berl. 1990. Effects of prostacyclin on the cAMP system in cultured rat inner medullary collecting duct cells. *Am. J. Physiol.* 258:F1218–F1223.

48. Wesson, D.E. 1996. Prostacyclin increases distal tubule HCO_3 secretion in the rat. *Am J. Physiol.* 271:F1183–F1192.

49. Korbmacher, C., E. Boulpaep, G. Giebisch, and J. Geibel. 1993. Endothelin increases $[Ca^{2+}]_i$ in M-1 mouse cortical collecting duct cells by a dual mechanism. *Am. J. Physiol.* 265:C349–C357.

50. Simonson, M.S., S. Wann, P. Mene, G.R. Dubyak, M. Kester, Y. Nakazato, J.R. Sedor, and M.J. Dunn. 1989. Endothelin stimulates phospholipase C, Na^+/K^+ exchange, c-fos expression and mitogenesis in rat mesangial cells. *J. Clin. Invest.* 83:708–712.

51. Tsukahara, H., H. Ende, H.I. Magazine, W.F. Bahou, and M.S. Goligorsky. 1994. Molecular and functional characterization of the non-isopeptide-selective ETB receptor in endothelial cells. Receptor coupling to nitric oxide synthase. *J. Biol. Chem.* 269:21778–21785.